NEUROSCIENCE
RESEARCH ARTICLE
M. Xu et al. / Neuroscience 544 (2024) 28–38

Electroacupuncture Enhances the Functional Connectivity of Limbic System to Neocortex in the 5xFAD Mouse Model of Alzheimer's Disease

Mingzhu Xu,[a,*] Run Lin,[b] Huaneng Wen,[a,c] Yixiao Wang,[b] John Wong,[d] Zhihua Peng,[b] Lu Liu,[a] Binbin Nie,[e] Jing Luo,[b] Xiaoyu Tang[b] and Shaoyang Cui[b,*]

[a] *Department of Rehabilitation Medicine, Shenzhen Hospital, Southern Medical University, Shenzhen 518100, China*

[b] *Shenzhen Hospital of Guangzhou University of Chinese Medicine (Futian), Shenzhen 518034, China*

[c] *The Third School of Clinical Medicine, Southern Medical University, Guangzhou, China*

[d] *MGH Institute of Health Professions, Boston, MA, USA*

[e] *Beijing Engineering Research Center of Radiographic Techniques and Equipment, Institute of High Energy Physics, Chinese Academy of Sciences, Beijing 100000, China*

Abstract—Our previous study revealed that acupuncture may exhibit therapeutic effects on Alzheimer's disease (AD) through the activation of metabolism in memory-related brain regions. However, the underlying functional mechanism remains poorly understood and warrants further investigation. In this study, we used resting-state functional magnetic resonance imaging (rsfMRI) to explore the potential effect of electroacupuncture (EA) on the 5xFAD mouse model of AD. We found that the EA group exhibited significant improvements in the number of platforms crossed and the time spent in the target quadrant when compared with the Model group ($p < 0.05$). The functional connectivity (FC) of left hippocampus (Hip) was enhanced significantly among 12 regions of interest (ROIs) in the EA group ($p < 0.05$). Based on the left Hip as the seed point, the rsfMRI analysis of the entire brain revealed increased FC between the limbic system and the neocortex in the 5xFAD mice after EA treatment. Additionally, the expression of amyloid-β(Aβ) protein and deposition in the Hip showed a downward trend in the EA group compared to the Model group ($p < 0.05$). In conclusion, our findings indicate that EA treatment can improve the learning and memory abilities and inhibit the expression of Aβ protein and deposition of 5xFAD mice. This improvement may be attributed to the enhancement of the resting-state functional activity and connectivity within the limbic-neocortical neural circuit, which are crucial for cognition, motor function, as well as spatial learning and memory abilities in AD mice.

Key words: Alzheimer's disease, 5xFAD mice, functional magnetic resonance imaging, electroacupuncture, functional brain networks, limbic-neocortical neural circuit.

INTRODUCTION

Alzheimer's disease (AD) is a neurodegenerative disease associated with progressive loss of learning, memory, and cognitive function (Sengoku, 2020). AD is characterized by the accumulation of extracellular amyloid-β (Aβ) plaques and intracellular neurofibrillary tangles (Tiwari et al., 2019), accompanied by synaptic and neuronal loss in the cerebral cortex and certain subcortical regions. Numerous therapeutic approaches have been explored in the pursuit of effective treatments for AD patients. However, these interventions have demonstrated limited symptomatic benefits and primarily focus on palliative management. There is still no available treatment to stop or reverse the progression of AD (De Simone et al., 2020).

Acupuncture, an important treatment in complementary medicine (Cao et al., 2016), has been demonstrated in numerous studies to be effective in treating many neurologic diseases including AD. Acupuncture has positive effects on the cognition in AD patients by modulating neuronal signaling pathways related to apoptosis cell survival, and glucose metabolism (Xu et al., 2021). In addition, based on the findings of our previous

*Corresponding authors. Address: Shenzhen Hospital of Guangzhou University of Chinese Medicine (Futian), Shenzhen 518034, China (Shaoyang Cui). Department of Rehabilitation Medicine, Shenzhen Hospital, Southern Medical University, Shenzhen 518100, China (Mingzhu Xu).
E-mail addresses: xulcui123@126.com (M. Xu), herb107@126.com (S. Cui).

Abbreviations: AD, Alzheimer's disease; Aβ, amyloid-β; Cpu, caudate putamen; EA, electroacupuncture; FC, functional connectivity; Hip, hippocampus; NBS, network-based statistics; ROI, regions of interest; rsfMRI, resting-state functional magnetic resonance imaging.

https://doi.org/10.1016/j.neuroscience.2024.02.025
0306-4522/

positron emission tomography study (Cui et al., 2018a), acupuncture may positively affect cognition in AD model rats by increasing blood perfusion and ethylene glycol metabolism in certain brain regions. Moreover, electroacupuncture (EA) at specific acupoints may exert specific therapeutic effects (Xu et al., 2019). Previous studies have shown that "Three-needle Acupuncture for Intelligence" (*Zhisanzhen*) can significantly improve intelligence and cognitive function (Sun et al., 2018; Zhang et al., 2019; Zheng et al., 2021). However, the precise mechanism by which EA exerts its effects on the central nervous system in AD remains poorly understood and requires further investigation.

Biomarkers that precede common pathological and cognitive symptoms in animal models of AD may be useful for early screening and interventional treatment of AD. Resting-state functional magnetic resonance imaging (rsfMRI) is a non-invasive technique that enables the measurement of brain activity by quantifying the blood oxygen level-dependent signal, providing insights into neural activity before the onset of cognitive decline and brain structural atrophy. By investigating functional connectivity (FC) and spatiotemporal correlations between different brain regions, rsfMRI allows the evaluation of brain dysfunction based on neural connectivity networks. Numerous rsfMRI studies have demonstrated disruptions in amplitude flow frequency fluctuations, regional homogeneity, and interregional FC in AD (Wang et al., 2011; Xu et al., 2023; Chen et al., 2024). Significant amyloid plaque depositing due to FC deficits was also detected antecedently in animal model (Anckaerts et al., 2019), supporting the potential of rsfMRI as a non-invasive biomarker for detecting prodromal stages and underlying neuronal or synaptic dysfunction. On the other hand, another rsfMRI study (Qi et al., 2019; Lin et al., 2022) has indicated that EA can modulate the intrinsic functional structure of the brain, with particular emphasis on the limbic/paralimbic regions such as the amygdala, hippocampus (Hip), entorhinal cortex, and anterior cingulate gyrus, which have emerged as network hubs. One of the primary pathological features of AD is the abnormal deposition of Aβ, which exhibits synaptotoxic effects (Shah et al., 2016). Synaptic dysfunction can lead to a reduction in synaptic plasticity, which in turn affects brain network FC and may even result in the impairment of brain network FC (Vosoughi et al., 2020; Zeng et al., 2023). Aβ may propagate throughout the hip and cortex in AD mice at 6–7 months, coinciding with spatial and learning memory deficits as assessed by the Morris water maze (Crapser et al., 2020). The deposition of Aβ in the brain is associated with the FC of its neural networks (Tahmi et al., 2020). A distinct reduction in the FC of the brain networks in patients with mild cognitive impairment was also found compared to healthy adults, as evidenced by the analysis of the salience network (Yi et al., 2015). However, the relevance between Aβ deposition and FC of different brain regions remains inadequately comprehended.

Therefore, we used rsfMRI to investigate the effect of "Three-needle Acupuncture for Intelligence" combined with electrical stimulation on 6-month-old 5xFAD mouse model of AD to hypothesize that EA could enhance learning and memory abilities while attenuating Aβ deposition in AD mice by modulating or augmenting resting-state functional activity and connectivity within the limbic system, thus achieving the goal of effective treatment of AD (Fig. 1).

EXPERIMENTAL PROCEDURES

Ethical statement

All experiments involving animal were reviewed and approved by the Ethics Committee of Guangzhou University of Traditional Chinese Medicine on the Use of Live Animal in Teaching and Research (permit numbers 20221115003) in conformity to *The Guide* (Care and Animals, 2011). This study complied with internationally accepted standards and the three Rs principle (Replace, Reduce, Refine). All efforts were made to reduce the suffering of animal and to avoid increasing unnecessary use of mice.

Animals

Male 5xFAD-transgenic mice on a congenic C57BL/6 background were provided by the Cavens Laboratory Animal Co., Ltd. (Changzhou, China). These 5xFAD mice expressed a total of five AD-related mutations in the human APP and PSEN1 transgenes, including the Swedish (K670N/M671L), Florida (I716V) and London (V717I) mutations in APP, and the M146L and L286V mutations in PSEN1. In this study, mice (adult male, $n = 16$, ≈20 g, 5xFAD, postnatal day 180) were fed until 6 months old. All animals were maintained at 23 ± 2 °C and 60 ± 15% relative humidity with free access to feed and water.

EA stimulation

The specific experimental method of EA therapy has been described previously (Cui et al., 2018b). The 5xFAD mice were randomly divided into 2 groups (6 months old, $n = 8$ per group): EA-treated (EA group) and control untreated mice (Model group). After removal of hair around the acupoints to facilitate needle position, the skin was cleaned using alcohol swabs. The head of each mouse was then positioned on a stereotactic frame (RWD Life Science, 71000) with 2% isoflurane anesthetized (RWD Life Science, R510-22). The EA group received stainless steel needle (diameter 0.16 mm, length 5 mm) insertion into "Three-needle Acupuncture for Intelligence" acupoints (*GV24* located 1.3 mm directly above the midpoint of the mouse's eyes and bilateral *GB13* located 2 mm lateral to *GV24*) at an intensity level of 1 mA and a frequency of 2 Hz with a continuous wave mode by a stimulator (model SDZ-III, *Hwato*, Suzhou Medical Appliance Factory, China) for 15 min daily, 5 days weekly, 8 weeks. Previous studies using different animal models have shown positive effects of these specific acupoints in improving the learning and memory abilities (Cui et al., 2018b; Zhang et al., 2019). Moreover, EA-related studies have demonstrated that current parameters of 1 mA and 2 Hz are

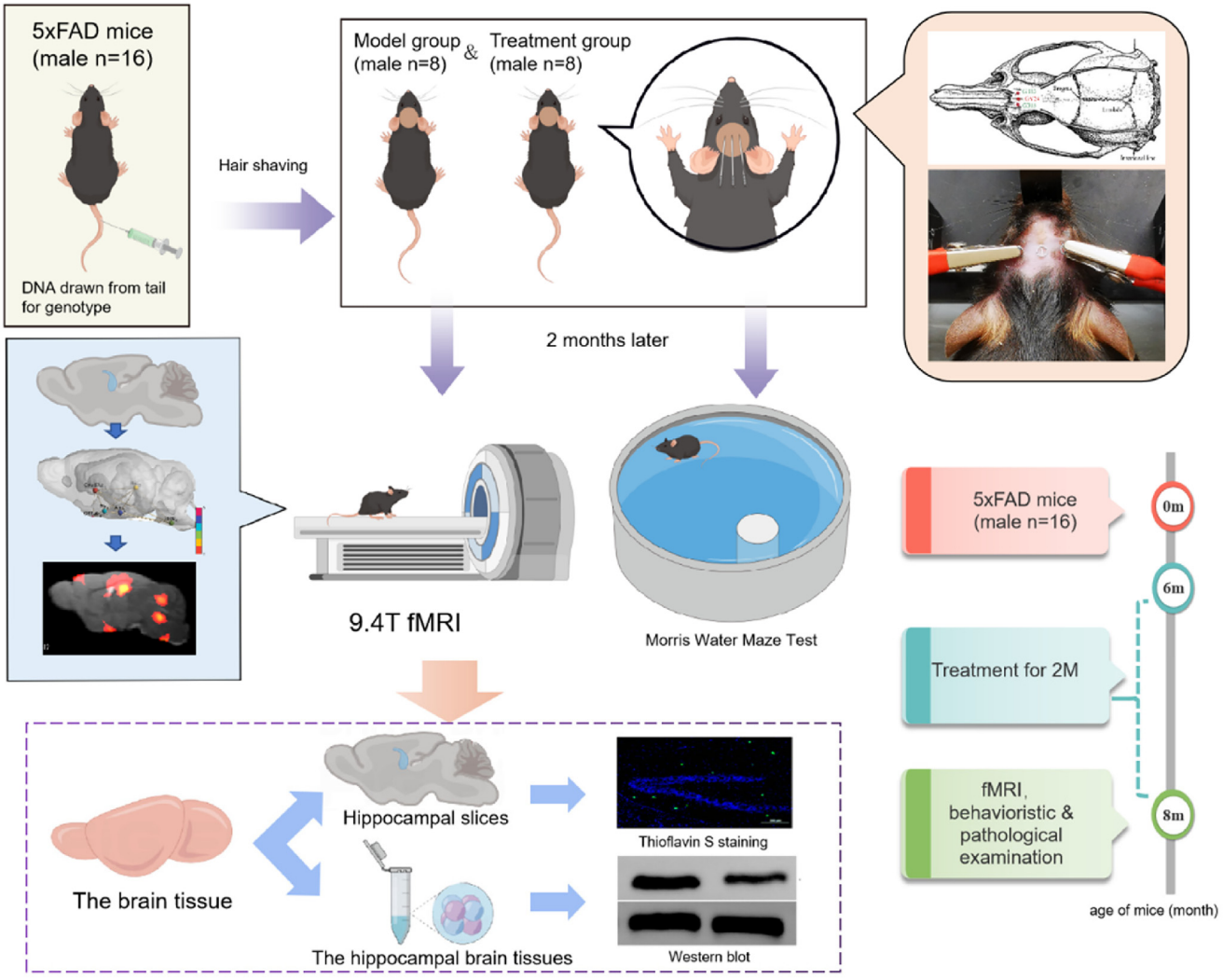

Fig. 1. Experimental flow diagram by Figdraw. (ID: IWAOR3335a).

effective in improving cognitive function (Cai et al., 2019). In addition, the treatment duration with EA is 15 min per day, conducted 5 days a week for a total of 8 weeks, has been proven to be effective in the treatment of AD (Cui et al., 2018b; Liang et al., 2021; Chen et al., 2023). The mice in the model group were fixed in the same way without EA stimulation for the same treatment cycle.

MRI animal preparation

Mice were first anesthetized with 3.5% isoflurane in a box for 5 min. After intubation, they were secured on a plastic cradle with a tooth bar and plastic screws in the ear canals. Throughout the MRI scanning process, mechanical ventilation was provided using a ventilator (TOPO, Kent Scientific Corp., Torrington, United States) delivering 0.4% isoflurane in room-temperature air, while dexmedetomidine at 0.04 mg/kg/h was subcutaneously injected to maintain sedation. In addition, pancuronium bromide (0.1 mg/kg) was intraperitoneally administered to reduce head movement. Real-time monitoring of rectal temperature was performed using a MRI-compatible animal heating system (Small-Animal Instrument, HEART, United States) and maintained at 37 ± 0.1 °C. Body temperature was regulated using a water circulation system maintaining a rectal temperature of 37.0 °C Physiological parameters were continuously measured using an MRI-compatible system (Small-Animal Instruments, Stony Brook, NY, United States). Vital signs remained within normal physiological range throughout the experiment, with a rectal temperature of 37.0 °C, heart rate of 350–420 beats/min, breathing rate of > 80–100 breaths/min, and oxygen saturation of ~95% as measured by pulse oximeter.

Resting-State functional MRI acquisition and processing

MRI scanning was performed on a 9.4 T scanner (Bruker Biospin, Germany) with a cryogenically cooled transmit and receive coil, controlled by a console running Paravision 6.0.1 (Bruker Biospin, Germany). Coregistration was performed using a T2 TurboRARE

anatomical image [TR = 3200 ms, TE = 33 ms, matrix size = 256 × 256, FOV = 16 × 16 mm^2, slice thickness = 400 μm, slices = 22, number of average = 2, resolution = 63.0 × 63.0 $μm^2$, RARE factor = 8]. RsfMRI was assessed via single-shot echo-planar imaging following local shimming using a gradient-echo echo-planar imaging sequence [FOV = 15 × 12 mm^2, slice thickness = 400 μm, slices = 22, data matrix = 75 × 60, TR = 1000 ms, TE = 15 ms, number of repetition = 360, bandwidth = 375 kHz, flip angle = 60°, resolution = 0.2 × 0.2 mm^2].

Statistical analysis

Statistical data of FC strength of brain network and recordings of electrophysiology were analyzed by two-way ANOVA, with Holm-Sidak correction for multiple comparisons ($p < 0.05$). Independent-samples T-test was used for to compare two groups, using a false discovery rate correction for multiple comparisons ($p < 0.05$) with a threshold of minimum 10 voxels.

RsfMRI data analysis

All image data processing was performed with the toolbox spmmouseIHEP[1] (Math Works, Natick, MA), SPM 12 (Welcome Department of Imaging Neuroscience, University College London; https://www.fil.ion.ucl.ac.uk/spm/) and the network-based statistics (NBS) toolbox (Zalesky et al., 2010). Sequences of MRI images were converted to NIFTI format, skull-stripped, and adjusted by a factor of ten before slice timing correction (Han et al., 2019). For each session, rsfMRI images were corrected for slice timing differences and realigned to the first volume using SPM12 affine transformation. Co-registered skull-stripped anatomical data were standardized into Paxinos and Franklin space (Franklin and Paxinos, 2004; Paxinos and Franklin, 2013), and the images were spatially smoothed using Gaussian kernel with a 3 mm full-width half maximum (FWHM). Motion correction denoising was consisted of 6 motion parameters (the first derivative, rotations and translation in 3 dimensions and the square of these six parameters). Temporal band-pass filtering was applied with cutoff frequencies set at 0.0007 (1/repetitions/3) Hz and 0.1 Hz (Janke and Ullmann, 2015; Manno et al., 2019). The images for analysis had to meet inclusion or exclusion criteria, including consistent normal vital signs throughout the entire scanning session with appropriate parameter settings (tidal volume, anesthetic dose, etc.), no image artifacts, and a maximum of 1 mm translation in the image realignment.

Seed-based correlation analysis (SCA): Six pairs of antecedently-based seeds were selected based on changes in anatomy or function (Lai et al., 2016; Lu et al., 2016; Cui et al., 2018a), including the caudate putamen (Cpu), Hip, insular cortex, piriform cortex, amygdala, olfactory tubercle. Between the reference time processes, Pearson's correlation coefficients were calculated on a voxel-wise basis to generate functional connective maps for each seed. These maps were subsequently Fisher z-transformed and compared using single-sample t-tests between two groups. To account for multiple comparisons, a family-wise error rate of $p < 0.05$ was corrected at the cluster level.

NBS: Based on the Paxinos Atlas, 68 ROIs were selected in toolbox spmmouseIHEP[1]. Z-scored Pearson's correlation coefficient between each time course extracted from ROI was used to generate the matrix. A permutation test was applied to identify suprathreshold connections for the identification of topological clusters using NBS, a cluster-statistical method that controls the error rate from family wise at the network level (Zalesky et al., 2010). To overcome the limitation of NBS, an effect size was calculated to perform a standard difference among edges. The effect size was used to calculate the combined effect size intra-module and inter-module, which took into account not only the effect size but also the proportion of effective edges to the overall in a module, revealing variation within and between modules. Modules with a greater than 1 effect size were considered significantly changed. The statistical analyses node modulation index was used to identify the most facilitated node to FC by averaging the total effect size of every single node, which was averaged between and within the modules (Zerbi et al., 2019). A graphical rsfMRI connectome analysis was executed to display the nodes of the network calculated by NBS in coronal and sagittal view as a translucent visualization of anatomy. The degree of the node was represented by its size. Gray nodes and edges showed the connectivity enhanced inter-module.

Morris water maze test

One week after the image acquisition, the hidden platform test was conducted in a Morris water maze to investigate spatial learning and memory ability. The water maze was a 60-cm-radius and 50-cm-deep circular pool, filled up with 24 °C milky water and divided into four quadrants with a diameter of 9 cm round platform hidden in the middle of the 4th quadrant, 2 cm below the surface in the pool. The training trial prior to probe trial was proceeding once a day for 5 days. To begin each trial, mice were positioned at a fixed place along the border of the pool and opposite the hidden platform. The animals were allowed to swim aimlessly before landing on the platform. Trajectory path was monitored and recorded with a camera to identify the times spent in the target quadrant and the numbers of platforms crossed.

Tissue processing

After completion of the image acquisition and behavioristics tests, mice were anesthetized by intraperitoneal injection of sodium pentobarbital and perfused with 4% paraformaldehyde until their tails became hard. After removal, three of the brains were selected randomly and fixed in 4% paraformaldehyde overnight, and then dehydrated with sucrose solution (15% and 30% sucrose solution), placed in the −80 °C refrigerator and be prepared to slice. The left Hip that revealed statistically significant difference after rsfMRI data analysis was chosen for the subsequent Western blot and Thioflavin S staining experiments.

Western blot

The Hip tissues were collected from each experimental group and lysed in 1 mL of RIPA protein lysis solution that contained a protease inhibitor. After grinding, the samples were incubated at 4 °C for 30 min and then centrifuged at 12,000 r/min for 15 min. The protein concentration of each sample was determined using the BCA (bicinchoninic acid) method and stored separately. An 8–10% polyacrylamide gel was prepared, and 5 μL of the sample was loaded for SDS-PAGE electrophoresis. The protein was then electrotransferred onto a 0.45-μm PVDF membrane and blocked with 5% skim milk powder at room temperature for 1 h. Antibodies diluted with skim milk powder were added, and the samples were incubated overnight at 4 °C. After sufficient washing, a 1:5000 dilution of HRP-labeled goat anti-rabbit secondary antibody was added and incubated at room temperature for 2 h. Finally, exposure and development were performed using an ECL luminescence kit, and density analysis was conducted using Image J software. Antibody information: GAPDH (1:2000, Servicebio, Wuhan, China), Aβ (1:1000, biorbyt, Britain).

Thioflavin S staining

Hip slices were frozen at room temperature and subjected to histochemical staining. Moisture content was controlled, and circles were drawn on the slices using a histochemical brush. After incubation in a filtered sulfur dye solution (0.3% in 50% alcohol) at room temperature for 8 min, the slides were washed with 80% alcohol for 10 s, followed by immersion in pure water for 10 s and a final rinse. 4′-6-diamidino-2-phenylindole (DAPI) staining solution was added dropwise and incubated in the dark at room temperature for 1 h. The slides were placed in PBS (PH 7.4) and shaken on a decolorization shaker and washed 3 times, each time for 5 min. Finally, after the slides were mounted using an anti-fluorescence quenching sealing agent, images were taken and observed under a fluorescence microscope.

RESULTS

EA enhanced the learning and memory function in 5xFAD mice

The number of platforms crossed ($t = -2.873$, df = 14, $p = 0.011$) and the time spent in target quadrant ($t = -2.545$, df = 14, $p = 0.022$) were both promoted in EA group compared with Model group (Fig. 2).

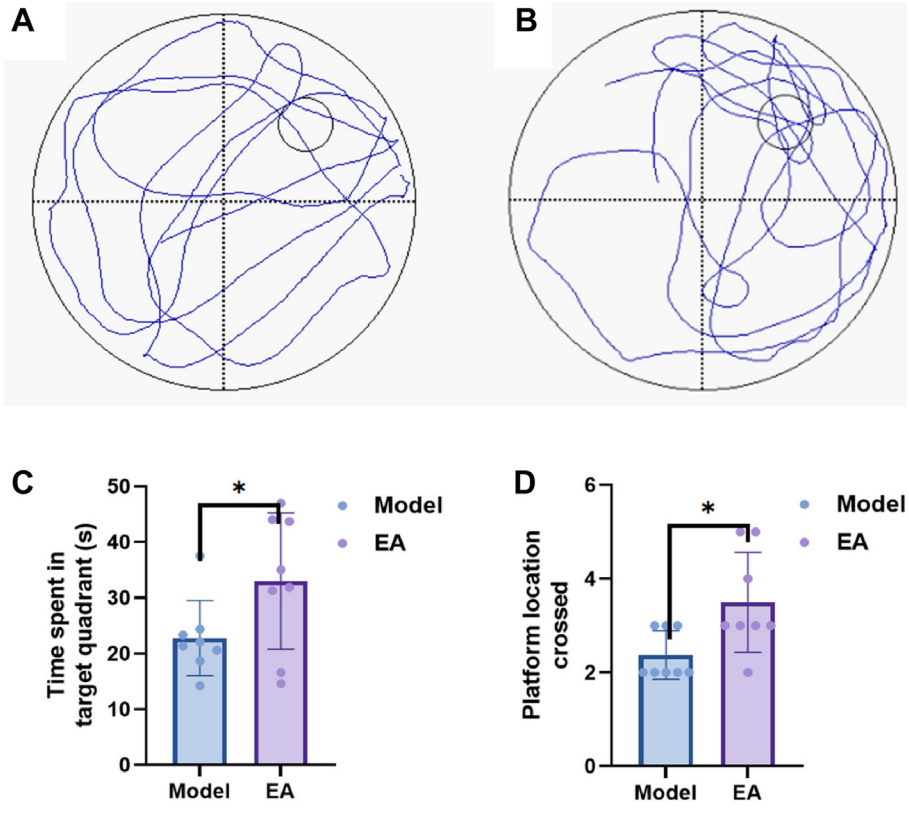

Fig. 2. EA treatment enhanced the time spent in target quadrant and the number of platforms crossed. (**A**) Representative Morris water maze motion trajectory diagram of the Model group; (**B**) Representative Morris water maze motion trajectory diagram of the EA group; (**C**) Quantification of times spent in the target quadrant. *$p < 0.05$, EA vs. Model analyzed by independent-samples t-test; (**D**) Quantification of number of platforms crossed. *$p < 0.05$, EA vs. Model analyzed by independent-samples t-test. *$p < 0.05$ compared with Model group. EA = Electroacupuncture.

EA treatment enhanced brain network FC calculated by NBS

Twelve brain regions were selected as ROIs according to previous studies. The functional connection signals of bilateral Hip and right insular cortex were enhanced among 12 ROIs with an increasing trend in the EA group compared with the same-month-age Model group with a significant difference, including the left Hip ($t = -2.132$, df = 190, $p = 0.034$) which was the most active region (Fig. 3).

Resting-State functional changes resulting from EA treatment

Based on the seed points of the left Hip, the correlation map with the whole brain voxel in time series was plotted, with the color map obtained after applying the threshold. The seed-based correlation analysis found that the FC of the left Hip increased significantly ($p = 0.049$, k = 100 voxels, Ke = 1108, Max-T = 3.3944). The changes also appeared in the right Hip ($p = 0.049$, k = 100 voxels, Ke = 2328, Max-T = 3.0582), left motor cortex ($p = 0.049$, k = 100

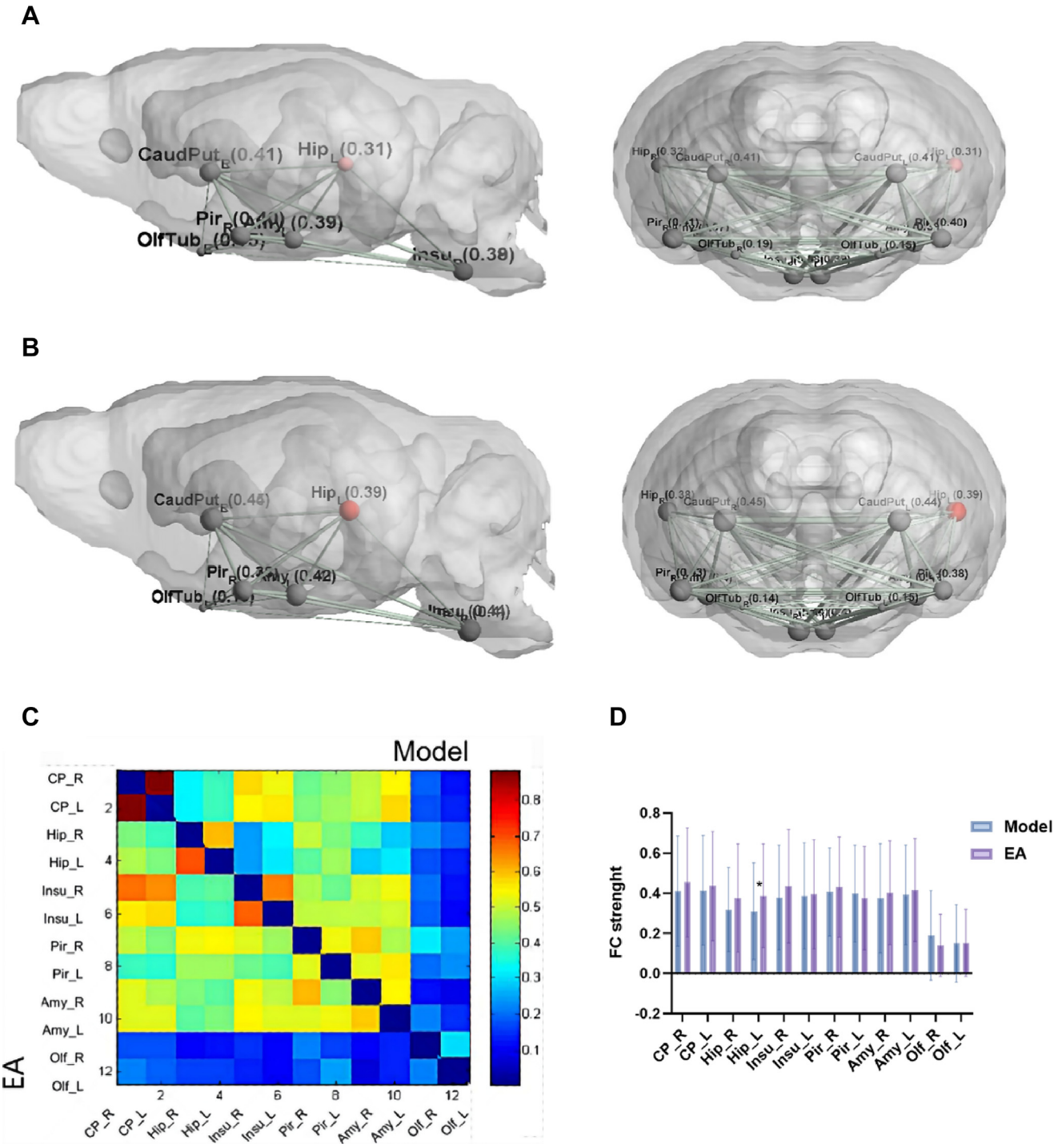

Fig. 3. Active regions increased in 5xFAD mice from EA treatment. (**A**) Anatomical visualization of a network calculated by NBS, viewed in coronal and sagittal planes (Model group); (**B**) Anatomical visualization of a network calculated by NBS, viewed in coronal and sagittal planes (EA group). The size of the node represents the degree of the node (i.e., the number of edges connected with one node in the network). Node and edges are color-coded within-module connections, gray nodes and edges are the enhanced connectivity between modules. (**C**) Heatmap of FC Mean-Rmatrix; (**D**) FC strength of Mean-Rmatrix, *$p < 0.05$. *$p < 0.05$ compared with Model group. EA = Electroacupuncture.

voxels, Ke = 1202, Max-T = 3.6005), right motor cortex (p = 0.049, k = 100 voxels, Ke = 1182, Max-T = 3.5515), right Cpu (p = 0.049, k = 100 voxels, Ke = 1781, Max-T = 3.2094), left somatosensory cortex (p = 0.049, k = 100 voxels, Ke = 1365, Max-T = 3.7852) and right temporal cortex (p = 0.049, k = 100 voxels, Ke = 1009, Max-T = 3.0498) (Fig. 4).

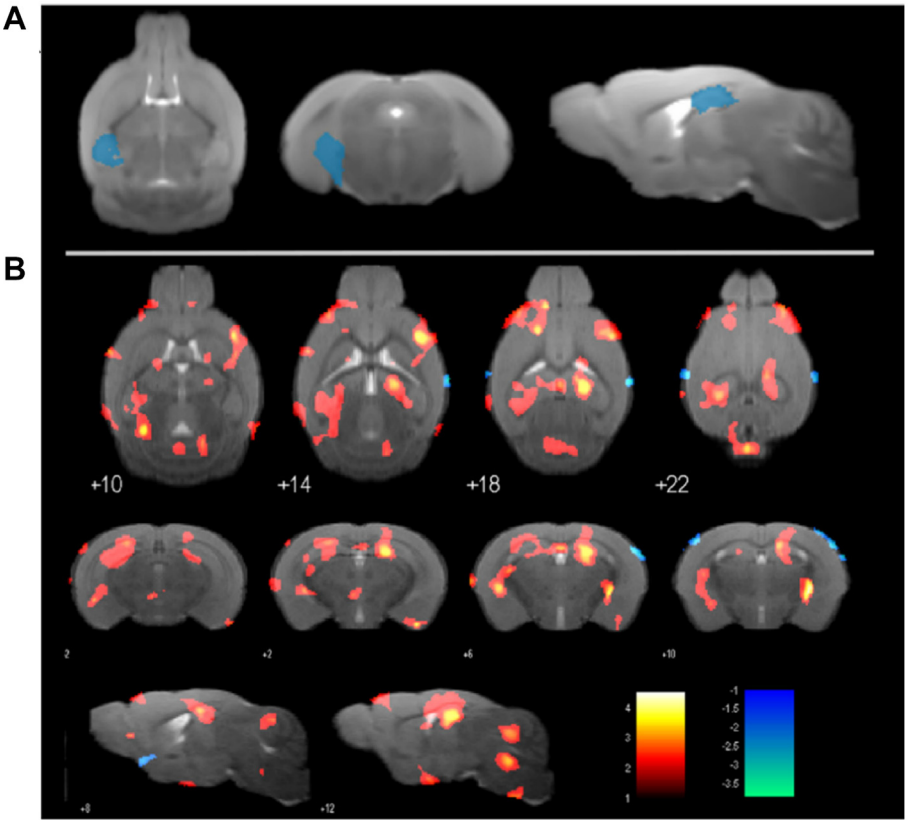

Fig. 4. Resting-state functional alterations from EA treatment. (**A**) Blue area is the left hippocampal seed spot as ROI; (**B**) The rsfMRI connectivity change after EA compared with the Model group. Color bar represents the strength of FC. The colour scale represents the T-value i.e. the strength of functional correlation with the left Hip. Hip = hippocampus. FC = functional connectivity.

EA inhibited the expression of Aβ protein and deposition in Hip

The impact of EA on Aβ protein deposition in the Hip of 5xFAD mice was further investigated in this study. Compared to the Model group, a significant reduction in the expression and distribution of Aβ protein deposition was observed after EA treatment (Fig. 5(**A,C**)). Moreover, the expression of Aβ protein in the EA group showed a decreasing trend compared to the Model group (Fig. 5(**B**)). These results strongly suggest that the improvement in cognitive function of 5xFAD mice after EA treatment may be attributed to the effective inhibition of the production and accumulation of Aβ protein in the Hip by EA.

DISCUSSION

Compared with other animal models of AD, such as 3xTg-AD mice, 6-month-old 5xFAD mice exhibit cortical neuronal and synaptic loss (Delgado-Peraza et al., 2021). Aβ deposition could be observed in neurons as early as 1.5 months old in 5xFAD mice, with subsequent dissemination of amyloid plaques throughout the Hip and cortex by 6–7 months, leading to spatial and learning memory deficits as demonstrated in the Morris water maze (Crapser et al., 2020). Additionally, the utilization of in vitro fertilization in the breeding of 5xFAD mice, based on advancements in genetic mouse breeding technology, offers a more efficient and cost-effective alternative to the natural breeding process for 3xTg-AD mice. Previous studies have shown that the 5xFAD transgenic mice were significant models of intraneuronal $A\beta_{42}$-induced neurodegeneration and amyloid plaque formation by reproducing the main pathological features of amyloid protein in AD (Kosel et al., 2020). Therefore, 6-month-old 5xFAD mice were selected as the AD animal model in this study.

Acupuncture has been used in the treatment of AD in Traditional Chinese Medicine for thousands of years. "Three-needle Acupuncture for Intelligence" originates from Jin's three-needle acupuncture therapy is a popular acupuncture technique created by *Rui Jin*, a famous doctor in Guangdong, that has been widely used in China to treat AD in the past decades for its simple and easy manipulation. "Three-needle Acupuncture for Intelligence" consists of GV24 (*Shenting*) and bilateral GB13 (*Benshen*), acupoints that have been associated with the clinical promotion of the intelligence level and cognitive function of patients with AD (Sun et al., 2018). In this study, "Three-needle Acupuncture for Intelligence" plus electrical stimulation on the 5xFAD mouse model of AD were used to investigate whether EA enhanced learning and memory capabilities and inhibited Aβ deposition in AD mice. Specifically, we aimed to elucidate the underlying mechanism by which EA modulates the resting-state functional activity and connectivity within the limbic-neocortex neural circuit.

The results of this study showed that EA could effectively improve the spatial learning and memory ability ($p < 0.05$) and inhibit Aβ deposition in the Hip of 5xFAD mice ($p < 0.05$), while the rsfMRI analysis indicated that EA promoted the left Hip FC to the right Hip, right Cpu, right motor cortex, left somatosensory cortex and right temporal cortex ($p < 0.05$), some of which are key components of the limbic system associated with learning and memory processes, while others represent neocortical structures encompassing the temporal lobe, posterior central gyrus of the parietal lobe, and precentral gyrus of the frontal lobe. The Morris water maze, long-established for assessing Hip-dependent learning capabilities, is a pivotal tool in the validation of rodent models of neurocognitive disorders, including AD (Bromley-Brits et al., 2011)). EA treatment has been found to markedly enhance the duration of stay in the target quadrant and the frequency of crossing the

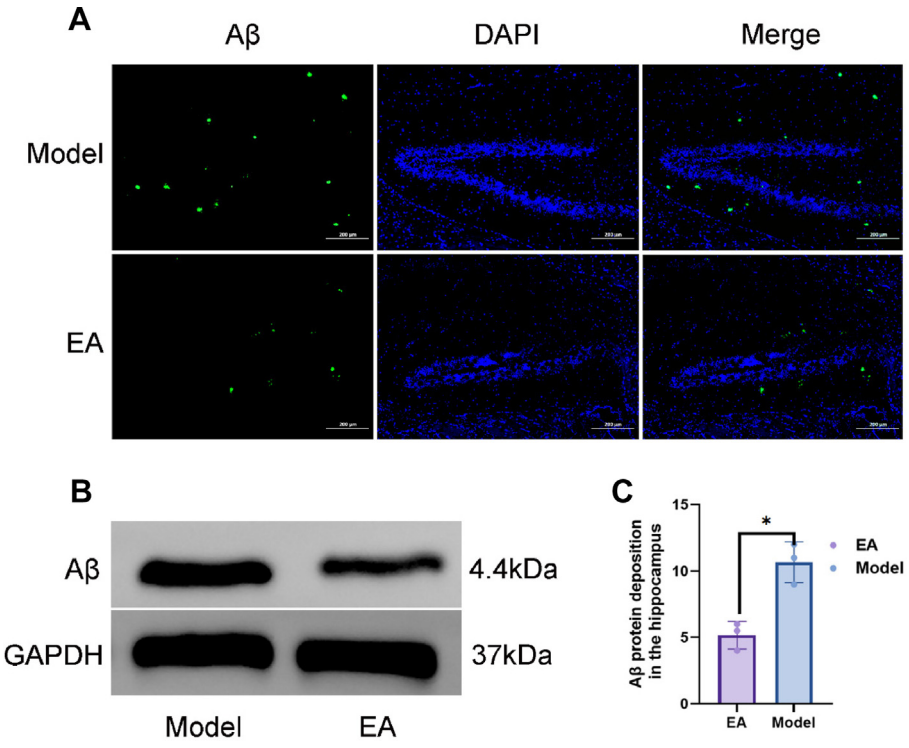

Fig. 5. EA inhibits Aβ protein and deposition in the Hip of 5xFAD mice. (**A**) Representative images for Aβ protein deposition in the Hip of Thioflavin S staining; (**B**) Representative western blot images for Aβ in the Hip. The expression of Aβ in the Hip was significantly decreased after treatment with EA compared to the Model group: (**C**) Statistic analysis for Aβ protein deposition in the Hip of Thioflavin S staining. Scale bar = 200 μm, *$p < 0.05$ compared with Model group. EA = Electroacupuncture. Hip = hippocampus.

target platform in 5xFAD mice, and significantly improved motor function and cognitive ability (Ni et al., 2023). The pathological presentation of Aβ deposition impacts the input of Hip memory-related signals and their output to the cortex (Thangavel et al., 2008), whereas EA treatment has been demonstrated to effectively inhibit the deposition of Aβ protein, thereby alleviating the pathological symptoms (Ding et al., 2023). In addition, several studies (Thal et al., 2002; Trejo-Lopez et al., 2022) have proposed a link between AD-related pathological changes, such as Aβ deposition and the progression of neurofibrillary tangles, with the intricate involvement of both the limbic structure and neocortex.

The limbic system, comprising a collection of brain structures situated laterally to the thalamus, beneath the cerebral cortex and above the brainstem, plays a vital role in modulating our behavioral and emotional responses, particularly those associated with survival behaviors such as feeding, reproduction, caring, and fight or flight responses (Torrico and Abdijadid, 2022). While our understanding of the intricate workings of the limbic system remains incomplete, advancements in neuroscience have enabled investigations into its various components and their interconnections. Notably, the key constituents of this region include the Hip, cingulate gyrus, and amygdala, which collectively contribute to diverse cognitive processes encompassing spatial memory, learning, motivation, emotional processing, and social cognition (Qi et al., 2019). Consequently, damage to specific regions within the limbic system can manifest as distinct clinical conditions. Recent research has highlighted the presence and deposition of Aβ and tau protein in limbic regions such as the Hip, entorhinal cortex, subiculum, amygdala, and cingulate gyrus (Gonzalez-Rodriguez et al., 2021; Trejo-Lopez et al., 2022), suggesting a potential association between the limbic system and the underlying pathological mechanisms of AD.

The neocortex, a highly intricate brain structure, governs a wide array of higher-order functions, including sensory perception, emotion, and cognition (Goebbels et al., 2006; Li et al., 2021a; Xing et al., 2021) is suggested to be involved in memory storage and retrieval based on the index of Hip (Kaefer et al., 2022). Motor deficits are some of the most prevalent non-cognitive symptoms of AD with patients showing impairments in speech, gait and fine motor skills. Several studies utilizing transcranial magnetic stimulation have proposed a correlation between reduced motor cortical excitability and the severity of cognitive impairment in AD (Alagona et al., 2001; Li et al., 2021b). Relevant researches have shown that the cellular damage to the motor cortex during the intermediate stage of AD can impact motor function, thereby influencing disease progression (Garvock-de et al., 2019; Orta-Salazar et al., 2019). In a recent study (Long et al., 2022), researchers explored an unconventional brain region outside the Hip, known as the somatosensory cortex, which lies beyond the traditional spatial navigation system. They discovered distinct head direction and angular head velocity cells within this region, suggesting its role as an inner compass for the brain. Accordingly, a hypothesis proposing the existence of a new spatial navigation system within the somatosensory cortex has been postulated. Additional studies have also found out that overproduction of Aβ in the somatosensory cortex was correlated with impairments of Hip long-term synaptic plasticity associated with the progression of AD and could be a bad influence on behavioral and functional measures (Stephen et al., 2010; Crouzin et al., 2013; D'Antonio et al., 2019; Tsui et al., 2022). Furthermore, investigations have highlighted the heightened vulnerability of the temporal cortex to neuropsychiatric and neurodegenerative disorders (Ueno et al., 2017), while gene expression stud-

ies have implicated the temporal cortex as an initiation site for the early stages of AD progression (Kumari et al., 2022).

Therefore, our experiment aimed to investigate the FC between the limbic system (specifically, the Hip and cingulate cortex) and the neocortex (including the motor cortex, somatosensory cortex, and temporal cortex) in AD mice subsequent to EA treatment. These findings indicate a potential therapeutic effect of EA treatment on spatial learning and memory abilities, as well as the inhibition of Aβ deposition, which may be significantly associated with the increased FC within the limbic-neocortical neural circuit, highlighting the importance of this circuit in driving cognition and memory processes.

This study demonstrated that EA can improve learning and memory abilities while inhibiting Aβ deposition in 5xFAD mice. The observed functional changes based on left Hip as the seed point in the entire brain regions of 5xFAD mice following EA treatment suggest that the neuromodulatory mechanism of EA may involve the enhancement of resting-state functional activity and connectivity within the limbic - neocortical neural circuit. Additionally, this circuit is likely to play a significant role in the deposition of Aβ in the Hip, as well as cognition, motor function, and spatial learning and memory abilities in AD mice. Evidence from this study also highlights the need for more attention to the association between the decline distribution of amyloid plaque and the connectivity within specific brain regions. Subsequent investigations will prioritize the examination of biomarkers within the neural circuitry of both the limbic system and neocortex.

ACKNOWLEDGEMENTS

All authors contributed to the study conception and design and critical revision of the article. MX and SC designed the research. RL, YW and XT implemented the experiment. MX, RL, JW and HW wrote and edited the manuscript. BN, RL and HW analyzed and plotted the data. LL, JL and ZP performed the research and data curation. All authors contributed to the article and approved the submitted version.

FUNDING

The study was supported by Natural Science Foundation of China (No. 81904275), Shenzhen Municipal Science, Technology and Innovation Commission (No. JCYJ20190814113801663), Chinese Medicine Key Medical Specialties Construction Project of Shenzhen Municipal Health Commission (Grant No. ZYTS019), and Research Foundation of Shenzhen Hospital of Southern Medical University (PT2019GZR08).

ETHICS APPROVAL

All experiments involving animal were reviewed and approved by the Ethics Committee of Guangzhou University of Traditional Chinese Medicine on the Use of Live Animal in Teaching and Research (permit numbers 20221115003). All protocols were conducted in adherence to the National Institutes of Health Guide for the Care and Use of Laboratory Animals. The reporting of the animal research experiments follows the Animal Research: Reporting of In Vivo Experiments, Version 2.0 (ARRIVE 20.0) guidelines.

DECLARATION OF COMPETING INTEREST

No competing interests.

REFERENCES

Alagona G, Bella R, Ferri R, Carnemolla A, Pappalardo A, Costanzo E, et al. (2001) Transcranial magnetic stimulation in Alzheimer disease: motor cortex excitability and cognitive severity. Neurosci Lett 314(1–2):57–60.

Anckaerts C, Blockx I, Summer P, Michael J, Hamaide J, Kreutzer C, et al. (2019) Early functional connectivity deficits and progressive microstructural alterations in the TgF344-AD rat model of Alzheimer's Disease: a longitudinal MRI study. Neurobiol Dis 124:93–107.

Bromley-Brits K, Deng Y, Song W (2011) Morris water maze test for learning and memory deficits in Alzheimer's disease model mice. J Vis Exp(53).

Cai M, Lee JH, Yang EJ (2019) Electroacupuncture attenuates cognition impairment via anti-neuroinflammation in an Alzheimer's disease animal model. J Neuroinflammation 16(1):264.

Cao Y, Zhang LW, Wang J, Du SQ, Xiao LY, Tu JF, et al. (2016) Mechanisms of acupuncture effect on alzheimer's disease in animal- based researches. Curr Top Med Chem 16(5):574–578.

Care NRCU, Animals AUOL (2011) Guide for the Care and Use of Laboratory Animals. Washington (DC): National Academies Press (US).

Chen HJ, Guo Y, Ke J, Qiu J, Zhang L, Xu Q, Zhong Y, Lu GM, Qin H, Qi R, Chen F (2024) Characterizing typhoon-related posttraumatic stress disorder based on multimodal fusion of structural, diffusion, and functional magnetic resonance imaging. Neuroscience 537:141–150.

Chen Y, Li Y, Wu M, Li Z (2023) Electroacupuncture improves cognitive function in APP/PS1 mice by inhibiting oxidative stress related hippocampal neuronal ferroptosis. Brain Res 148744.

Crapser JD, Spangenberg EE, Barahona RA, Arreola MA, Hohsfield LA, Green KN (2020) Microglia facilitate loss of perineuronal nets in the Alzheimer's disease brain. EBioMedicine 58 102919.

Crouzin N, Baranger K, Cavalier M, Marchalant Y, Cohen-Solal C, Roman FS, et al. (2013) Area-specific alterations of synaptic plasticity in the 5XFAD mouse model of Alzheimer's disease: dissociation between somatosensory cortex and hippocampus. PLoS One 8(9):e74667.

Cui S, Xu M, Huang J, Wang QM, Lai X, Nie B, et al. (2018) Cerebral responses to acupuncture at GV24 and bilateral GB13 in rat models of Alzheimer's disease. Behav Neurol 8740284.

Cui S, Xu M, Huang J, Wang QM, Lai X, Nie B, et al. (2018b) Cerebral Responses to Acupuncture at GV24 and Bilateral GB13 in Rat Models of Alzheimer's Disease. Behav Neurol 8740284.

D'Antonio F, De Bartolo MI, Ferrazzano G, Trebbastoni A, Amicarelli S, Campanelli A, et al. (2019) Somatosensory Temporal Discrimination Threshold in Patients with Cognitive Disorders. J Alzheimers Dis 70(2):425–432.

De Simone A, Naldi M, Tedesco D, Bartolini M, Davani L, Andrisano V (2020) Advanced analytical methodologies in Alzheimer's disease drug discovery. J Pharm Biomed Anal 178 112899.

Delgado-Peraza F, Nogueras-Ortiz CJ, Volpert O, Liu D, Goetzl EJ, Mattson MP, et al. (2021) Neuronal and astrocytic extracellular vesicle biomarkers in blood reflect brain pathology in mouse models of alzheimer's disease. Cells 10(5).

Ding Y, Li L, Wang S, Cao Y, Yang M, Dai Y, et al. (2023) Electroacupuncture promotes neurogenesis in the dentate gyrus

and improves pattern separation in an early Alzheimer's disease mouse model. Biol Res 56(1):65.
Franklin KBJ, Paxinos G (2004) The mouse brain in stereotaxic coordinates. Compact 2nd ed. Amsterdam; Boston: Elsevier Academic Press.
Garvock-de MT, Fertan E, Stover K, Brown RE (2019) Motor deficits in 16-month-old male and female 3xTg-AD mice. Behav Brain Res 356:305–313.
Goebbels S, Bormuth I, Bode U, Hermanson O, Schwab MH, Nave KA (2006) Genetic targeting of principal neurons in neocortex and hippocampus of NEX-Cre mice. Genesis 44(12):611–621.
Gonzalez-Rodriguez M, Astillero-Lopez V, Villanueva-Anguita P, Paya-Rodriguez ME, Flores-Cuadrado A, Villar-Conde S, et al. (2021) Somatostatin and Astroglial Involvement in the Human Limbic System in Alzheimer's Disease. Int J Mol Sci 22(16).
Han Z, Chen W, Chen X, Zhang K, Tong C, Zhang X, et al. (2019) Awake and behaving mouse fMRI during Go/No-Go task. NeuroImage 188:733–742.
Janke AL, Ullmann JF (2015) Robust methods to create ex vivo minimum deformation atlases for brain mapping. Methods (San Diego, Calif.) 73:18–26.
Kaefer K, Stella F, McNaughton BL, Battaglia FP (2022) Replay, the default mode network and the cascaded memory systems model. Nat Rev Neurosci 23(10):628–640.
Kosel F, Pelley J, Franklin TB (2020) Behavioural and psychological symptoms of dementia in mouse models of Alzheimer's disease-related pathology. Neurosci Biobehav Rev 112:634–647.
Kumari A, Rahaman A, Zeng XA, Farooq MA, Huang Y, Yao R, et al. (2022) Temporal cortex microarray analysis revealed impaired ribosomal biogenesis and hyperactivity of the glutamatergic system: an early signature of asymptomatic alzheimer's disease. Front Neurosci 16 966877.
Lai X, Ren J, Lu Y, Cui S, Chen J, Huang Y, et al. (2016) Effects of acupuncture at HT7 on glucose metabolism in a rat model of Alzheimer's disease: an 18F-FDG-PET study. Acupunct Med: J Brit Med Acupunct Soc(3):215–222.
Li X, Guo S, Xu S, Chen Z, Wang L, Ding J, et al. (2021a) Neocortex- and hippocampus-specific deletion of Gabrg2 causes temperature-dependent seizures in mice. Cell Death Dis 12(6):553.
Li X, Qi G, Yu C, Lian G, Zheng H, Wu S, et al. (2021b) Cortical plasticity is correlated with cognitive improvement in Alzheimer's disease patients after rTMS treatment. Brain Stimul 14 (3):503–510.
Liang PZ, Li L, Zhang YN, Shen Y, Zhang LL, Zhou J, et al. (2021) Electroacupuncture Improves clearance of amyloid-beta through the glymphatic system in the SAMP8 mouse model of alzheimer's disease. Neural Plast 2021 9960304.
Lin B, Zhang L, Yin X, Chen X, Ruan C, Wu T, et al. (2022) Modulation of entorhinal cortex-hippocampus connectivity and recognition memory following electroacupuncture on 3×Tg-AD model: Evidence from multimodal MRI and electrophysiological recordings. Front Neurosci 16 968767.
Long X, Deng B, Young CK, Liu GL, Zhong Z, Chen Q, et al. (2022) Sharp tuning of head direction and angular head velocity cells in the somatosensory cortex. Adv Sci (Weinh) 9(14):e2200020.
Lu Y, Ren J, Cui S, Chen J, Huang Y, Tang C, et al. (2016) Cerebral glucose metabolism assessment in rat models of alzheimer's disease: an 18F-FDG-PET study. Am J Alzheimers Dis Other Demen 31(4):333–340.
Manno F, Isla AG, Manno S, Ahmed I, Cheng SH, Barrios FA, et al. (2019) Early stage alterations in white matter and decreased functional interhemispheric hippocampal connectivity in the 3xTg mouse model of alzheimer's disease. Front Aging Neurosci 11:39.
Ni H, Ren J, Wang Q, Li X, Wu Y, Liu D, et al. (2023) Electroacupuncture at ST 36 ameliorates cognitive impairment and beta-amyloid pathology by inhibiting NLRP3 inflammasome activation in an Alzheimer's disease animal model. Heliyon 9(6): e16755.
Orta-Salazar E, Feria-Velasco AI, Díaz-Cintra S (2019) Primary motor cortex alterations in Alzheimer disease: A study in the 3xTg-AD model. Neurologia (Engl Ed) 34(7):429–436.
Paxinos G, Franklin KBJ (2013) Paxinos and Franklin's The mouse brain in stereotaxic coordinates, fourth ed.
Qi Z, An Y, Zhang M, Li HJ, Lu J (2019) Altered cerebro-cerebellar limbic network in AD spectrum: a resting-state fMRI study. Front Neural Circuits 13:72.
Sengoku R (2020) Aging and Alzheimer's disease pathology. Neuropathology 40(1):22–29.
Shah D, Praet J, Latif HA, Hofling C, Anckaerts C, Bard F, et al. (2016) Early pathologic amyloid induces hypersynchrony of BOLD resting-state networks in transgenic mice and provides an early therapeutic window before amyloid plaque deposition. Alzheimers Dement 12(9):964–976.
Stephen JM, Montaño R, Donahue CH, Adair JC, Knoefel J, Qualls C, et al. (2010) Somatosensory responses in normal aging, mild cognitive impairment, and Alzheimer's disease. J Neural Transm (Vienna) 117(2):217–225.
Sun W, Li M, Lin T, Sun Z, Xie Y, Ji S, et al. (2018) Effect of acupuncture at 3-points for intelligence on vascular dementia: Protocol for a systematic review and meta-analysis of randomized controlled trials. Medicine (Baltimore) 97(42):e12892.
Tahmi M, Rippon B, Palta P, Soto L, Ceballos F, Pardo M, et al. (2020) Brain amyloid burden and resting-state functional connectivity in late middle-aged hispanics. Front Neurol 11 529930.
Thal DR, Rüb U, Orantes M, Braak H (2002) Phases of A beta-deposition in the human brain and its relevance for the development of AD. Neurology 58(12):1791–1800.
Thangavel R, Van Hoesen GW, Zaheer A (2008) Posterior parahippocampal gyrus pathology in Alzheimer's disease. Neuroscience 154(2):667–676.
Tiwari S, Atluri V, Kaushik A, Yndart A, Nair M (2019) Alzheimer's disease: pathogenesis, diagnostics, and therapeutics. Int J Nanomedicine 14:5541–5554.
Torrico TJ, Abdijadid S (2022) *Neuroanatomy, Limbic System*. Treasure Island (FL): StatPearls Publishing.
Trejo-Lopez JA, Yachnis AT, Prokop S (2022) Neuropathology of Alzheimer's disease. Neurotherapeutics 19(1):173–185.
Tsui KC, Roy J, Chau SC, Wong KH, Shi L, Poon CH, et al. (2022) Distribution and inter-regional relationship of amyloid-beta plaque deposition in a 5xFAD mouse model of Alzheimer's disease. Front Aging Neurosci 14 964336.
Ueno H, Suemitsu S, Murakami S, Kitamura N, Wani K, Okamoto M, et al. (2017) Postnatal development of GABAergic interneurons and perineuronal nets in mouse temporal cortex subregions. Int J Dev Neurosci 63:27–37.
Vosoughi A, Sadigh-Eteghad S, Ghorbani M, Shahmorad S, Farhoudi M, Rafi MA, et al. (2020) Mathematical models to shed light on amyloid-beta and tau protein dependent pathologies in Alzheimer's disease. Neuroscience 424:45–57.
Wang Z, Yan C, Zhao C, Qi Z, Zhou W, Lu J, et al. (2011) Spatial patterns of intrinsic brain activity in mild cognitive impairment and Alzheimer's disease: a resting-state functional MRI study. Hum Brain Mapp 32(10):1720–1740.
Xing L, Kubik-Zahorodna A, Namba T, Pinson A, Florio M, Prochazka J, et al. (2021) Expression of human-specific ARHGAP11B in mice leads to neocortex expansion and increased memory flexibility. EMBO J 40(13):e107093.
Xu J, Lin X, Cheng KK, Zhong H, Liu M, Zhang G, et al. (2019) Metabolic response in rats following electroacupuncture or moxibustion stimulation. Evid Based Complement Alternat Med 2019:6947471.
Xu J, Luo Y, Liu Y, Zhong L, Liu H, Zhang X, Cheng Q, Yang Z, Zhang Y, Weng A, Ou Z, Yan Z, Zhang W, Hu Q, Peng K, Liu G (2023) Neural correlates of facial emotion recognition impairment in blepharospasm: a functional magnetic resonance imaging study. Neuroscience 531:50–59.
Xu XJ, Yang MS, Zhang B, Niu F, Dong JQ, Liu BY (2021) Glucose metabolism: a link between traumatic brain injury and Alzheimer's disease. Chin J Traumatol 24(1):5–10.
Yi D, Choe YM, Byun MS, Sohn BK, Seo EH, Han J, et al. (2015) Differences in functional brain connectivity alterations associated

with cerebral amyloid deposition in amnestic mild cognitive impairment. Front Aging Neurosci 7:15.
Zalesky A, Fornito A, Bullmore ET (2010) Network-based statistic: identifying differences in brain networks. Neuroimage 53 (4):1197–1207.
Zeng T, Li J, Xie L, Dong Z, Chen Q, Huang S, et al. (2023) Nrf2 regulates iron-dependent hippocampal synapses and functional connectivity damage in depression. J Neuroinflammation 20 (1):212.
Zerbi V, Floriou-Servou A, Markicevic M, Vermeiren Y, Sturman O, Privitera M, et al. (2019) Rapid reconfiguration of the functional connectome after chemogenetic locus coeruleus activation. Neuron 103(4):702–718.
Zhang J, Tang C, Liao W, Zhu M, Liu M, Sun N (2019) The antiapoptotic and antioxidative stress effects of Zhisanzhen in the Alzheimer's disease model rat. Neuroreport 30(9):628–636.
Zheng X, Lin W, Jiang Y, Lu K, Wei W, Huo Q, et al. (2021) Electroacupuncture ameliorates beta-amyloid pathology and cognitive impairment in Alzheimer disease via a novel mechanism involving activation of TFEB (transcription factor EB). Autophagy 17(11):3833–3847.

(Received 1 September 2023, Accepted 24 February 2024)
(Available online 28 February 2024)